Effects of medicagenic acid metabolites, originating from biotransformation of an Herniaria hirsuta extract, on calcium oxalate crystallization in vitro

Reference:
Peeters Laura, Foubert Kenn, Breynaert Annelies, Schreurs Gerd, Verhulst Anja, Pieters Luc, Hermans Nina.- Effects of medicagenic acid metabolites, originating from biotransformation of an Herniaria hirsuta extract, on calcium oxalate crystallization in vitro
Journal of ethnopharmacology - ISSN 1872-7573 - 285(2022), 114860
Full text (Publisher's DOI): https://doi.org/10.1016/J.JEP.2021.114860
To cite this reference: https://hdl.handle.net/10067/1833420151162165141

Effects of medicagenic acid metabolites, originating from biotransformation of an *Herniaria hirsuta* extract, on calcium oxalate crystallization *in vitro*

Laura Peeters [a]*, Kenn Foubert [a], Annelies Breynaert [a], Gerd Schreurs [b], Anja Verhulst [b], Luc Pieters [a] and Nina Hermans [a]

[a] Natural Products & Food Research and Analysis (NatuRA), University of Antwerp, Universiteitsplein 1, 2610 Antwerp, Belgium

[b] Laboratory of Pathophysiology, University of Antwerp, Universiteitsplein 1, 2610 Antwerp, Belgium

* Correspondence: laura.peeters@uantwerpen.be; Tel.: +32-3265-9096

Declarations of interest: none

Abstract

Ethnopharmacological relevance: Herniaria hirsuta is traditionally used in Moroccan folk medicine for treatment of urinary stones and as a diuretic. It is rich in saponins, which are known to be deglycosylated in the colon, whereafter aglycones such as medicagenic acid are absorbed and further metabolized in the liver.

Aim of the study: A sample of hepatic metabolites of medicagenic acid, with medicagenic acid glucuronide as the most abundant one, was evaluated for *in vitro* activity against urinary stones. A crystallization assay and a crystal-cell interaction assay were used to evaluate *in vitro* activity of hepatic metabolites of medicagenic acid on CaC_2O_4 (calciumoxalate) crystals, present in the majority of urinary stones.

Materials and methods: In the crystallization assay the effects on nucleation of Ca^{2+} and $C_2O_4^{2-}$ and aggregation of the CaC_2O_4 crystals are studied. In the crystal-cell interaction assay crystal retention is investigated by determining the amount of Ca^{2+} bound to injured monolayers of MDCK I cells.

Results: Results of the crystallization assay showed a tentative effect on crystal aggregation. The crystal-cell interaction assay showed a significant inhibition of crystal binding, which may reduce crystal retention in the urinary tract.

Conclusions: As both formation of crystals by inhibiting aggregation and retention of crystals is affected, the beneficial effect of *H. hirsuta* against urinary stones may at least in part be attributed to medicagenic acid metabolites, indicating that saponins containing medicagenic acid may act as prodrugs.

Keywords: *Herniaria hirsuta,* Caryophyllaceae, urolithiasis, crystallization, crystal-cell interaction

Abbreviations:

CaOx: calcium oxalate; CMC: critical micellar concentration; COM: calcium oxalate monohydrate; DMEM: dulbecco's modified eagle medium; LDH: lactate dehydrogenase MDCK: madin darby canin kidney cells; MDCK I: madin darby canin kidney cells, subtype I; NADPH RS: reduced nicotinamide adenine dinucleotide phosphate regenerating system; OD: optical density; SPE: solid phase extraction

Introduction

Urinary stone disease is considered as an economic burden of the health system as it affects approximately 10-15% of the population in the developed world and the incidence can be as high as 20-25% in the Middle East with a peak at ages 20 to 40 years (Moe, 2006; Rule et al., 2014). The majority of urinary stones is formed in the kidney by a complex process which remains incompletely understood, but involves several steps which occur either sequentially or concurrently including supersaturation, nucleation, growth and aggregation (Sharma et al., 2016). The majority of stones are composed of calcium oxalate monohydrate (COM) crystals, representing about 67% of the stones for men and 75% for women (Alelign et al., 2018). Several studies demonstrated that crystals adhere more likely to apoptotic or necrotic cells, and to the surface of injured epithelial cells. (Alelign et al., 2018; Verkoelen et al., 1998).

The disease is characterized by its high recurrence rate, about 50% in 10 years and 75% in 20 years. Therefore, prevention of recurrence is crucial (Atmani et al., 2000). Several remedies are recommended, notwithstanding, there are no satisfactory drugs to cure and/or prevent kidney stone recurrences. During history many plant species have been used to treat stone diseases. A large number of species is described in many pharmacopeia all over the world, multiple of which are praised for their beneficial effects against both urinary stones and gallstones (Atmani, 2003). However, when investigating their active constituents, it should be considered that many natural products are prodrugs, e.g. glycosides, that are biotransformed and activated after oral administration (Butterweck and Nahrsteds, 2012).

72 An aqueous extract of the aerial parts of *Herniaria hirsuta* L. (Caryophyllaceae) is an
73 herbal medicine widely used against urolithiasis and which also has diuretic properties.
74 The European Medicines Agency (EMA) has accepted *Herniaria glabra* L., *H. hirsuta* L.
75 and *H. incana* Lam., herba as "traditional herbal medicinal product to increase the amount
76 of urine to achieve flushing of the urinary tract as an adjuvant in minor urinary
77 complaints" (EMA, 2018; EMA, 2020). Some ethnobotanical surveys proved the
78 traditional use of *H. hirsuta* in Morocco, Jordan, Palestine, Bosnia-Herzegovina and
79 Mallorca for the treatment of bladder disorder and as a renal lithotriptic (Ammor et al.,
80 2018). The beneficial effects of the extract have been demonstrated in several studies
81 (Aggarwal et al., 2014; Atmani, 2003; Atmani et al., 2004). Even though a lot of research
82 has been done to prove the activity of *H. hirsuta* against urolithiasis, little is known about
83 the active compounds and the exact mechanism of action. Previous phytochemical
84 research on *Herniaria* species revealed the presence of saponins, flavonoids and
85 coumarins (Charrouf et al., 1996; Mbark et al., 1995; MBark et al. 1996, van Dooren et
86 al., 2016; Peeters et al., 2020a). Literature suggests that the antilithiatic potential of *H.*
87 *hirsuta* is attributed to saponins or metabolites thereof (van Dooren et al., 2016).
88
89 Monitoring of metabolite formation during *in vitro* gastrointestinal biotransformation
90 studies of an extract of *H. hirsuta* showed an increase in formation of saponin aglycones,
91 with medicagenic acid as the most abundant one. Medicagenic acid was further
92 biotransformed in an *in vitro* hepatic model into several phase I and II metabolites
93 (Peeters et al., 2020a; Peeters et al., 2020b). The aim of this study was to evaluate the *in*
94 *vitro* effect of these metabolites on calcium oxalate crystallization and crystal-cell
95 interaction.

96

97 **Materials and methods**

98 Chemicals

99 Ultrapure water with a resistivity of 18.2 MΩ.cm at 25 °C was generated with a
100 Millipore™-purification system. UHPLC-grade methanol, acetonitrile and formic acid
101 were purchased from Biosolve (Dieuze, France). Medicagenic acid was provided by
102 Phytolab (Vestenbergsgreuth, Germany). Human liver S9 fraction and NADPH RS were
103 purchased from Tebu Bio (Boechout, Belgium). All other chemicals and biochemicals
104 were purchased from Sigma-Aldrich (St. Louis, USA).

105

106 Sample preparation

107 Liver biotransformation mimicking phase I and II reactions was performed using
108 medicagenic acid (Phytolab, Germany), the most abundant aglycone present in an extract
109 of *H. hirsuta* after gastrointestinal biotransformation. Hepatic biotransformation was
110 simulated *in vitro* by using pooled S9 fractions, previously described by Peeters et al.
111 (2020b).

112

113 Samples were purified by bringing 3 mL on a Chromabond® SPE C_{18} cartridge (500 mg)
114 (Machery-Nagel, Germany) preconditioned with MeOH and water. After sample
115 application, the column was successively rinsed with water and MeOH 30% (*v/v*).
116 Compounds were eluted with MeOH 100% (Theunis et al., 2007). The fraction was dried
117 under vacuum and stored at -80 °C. For more detailed information on the preparation of
118 the hepatic metabolites of medicagenic acid, see supporting information.

119

120 The purified sample of hepatic metabolites of medicagenic acid was redissolved in 40 µL
121 DMSO. The concentration of the most abundant metabolite present in the sample was
122 estimated with regard to the concentration of medicagenic acid before hepatic
123 biotransformation and the relative abundance of the metabolites. Approximately 30% of
124 medicagenic acid was biotransformed. Metabolites were previously identified using LC-
125 MS reporting medicagenic acid glucuronide as the most abundant metabolite, accounting
126 for (29.1 ± 1.7)% calculated relatively to the amount of medicagenic acid at t_0, resulting
127 in an approximate final concentration of 0.02 mM medicagenic acid glucuronide (Peeters
128 et al., 2020b). An overview of the hepatic biotransformation products of medicagenic acid
129 can be found in Figure 1 and Table 1S (supporting information).

130

131 Crystallization assay

132 Optical density of a suspension containing calcium and oxalate was monitored reflecting
133 the degree of crystallization, since optical density increases with increasing amounts of
134 crystals in suspension. The crystallization assay was based on two methods, previously
135 described in literature with small adaptations (Hess et al., 2000; Sharma et al., 2016).
136 Briefly, $CaCl_2$ and $Na_2C_2O_4$ solutions were prepared at a concentration of 2 mM in 10 mM
137 Tris (pH = 5.7). Solutions were filtered through a filter membrane with a pore diameter
138 of 0.22 µm (Whatman® Nuclepore™ Track-Etched Membranes, Sigma Aldrich, St.
139 Louis, MI, USA) and kept at room temperature. A volume of 1 mL oxalate solution was
140 transferred into a stirring cuvette with a 10 mm light path (Saillart, Antwerp, Belgium).
141 Then, 0.04 mL test compound was added, followed by 1 mL of calcium chloride solution.
142 The solution was continuously stirred in the cuvette at room temperature and optical

143 density was measured at 620 nm every 12 s for 20 min using an UV-VIS
144 spectrophotometer (Lambda 35 double beam, Perkin Elmer). The data were recorded
145 using the software program UV-WINLAB (version 6.2, Perkin Elmer).
146
147 An increase in optical density reflects an increase in particle number, in this case crystals,
148 in function of time as shown in Figure 2. When the upward slope of OD_{620} reaches its
149 maximum, the increase in turbidity mainly reflects an increase in particle number and
150 thus crystal nucleation. This slope is referred to as S_N. Subsequently, an equilibrium is
151 reached in which the solution has become saturated and crystal mass remains constant
152 (OD_{max}). Over time, a progressive decrease in OD_{620} is observed, which reflects the
153 decline in particle number due to crystal aggregation. The descending slope of OD_{620} over
154 time can be used as a measure for crystal aggregation, which is referred to as S_A (Hess et
155 al., 2000).
156
157 Sodium citrate was used as a positive control as it is able to form a complex with calcium
158 (Hess et al., 2000). Tested concentrations ranged from 0.3 mM to 0.5 mM and 0.7 mM
159 citrate (final concentration). The lowest concentration was based on the reaction of
160 calcium with citrate resulting in $Ca_3(C_6H_5O_7)_2$, taking 50% inhibition into account.
161
162 The level of inhibition was calculated as:
163 % Inhibition = $[1 - (S_{Ni} / S_{Nc})] \times 100$ for the rate of nucleation
164 % Inhibition = $[1 - (S_{Ai} / S_{Ac})] \times 100$ for the rate of aggregation
165 where c stands for control and i refers to the presence of an inhibitor. Negative inhibition
166 values indicate promotion of the respective crystallization process (Hess et al., 2000). The

167 effect was statistically evaluated using one-way ANOVA with Tukey post-hoc-test (IBM
168 SPSS Statistics version 27).
169
170 As a model compound for biotransformation products of saponins, aescin was used.
171 Aescin contains a monodesmosidic side chain showing structural resemblance with the
172 glucuronyl derivative of medicagenic acid, the main metabolite after hepatic
173 biotransformation. Different concentrations were tested based on the results of inhibiting
174 properties of citrate, including 0.35 mM and 0.7 mM, as a guidance to estimate a suitable
175 concentration for the mixture of hepatic metabolites of medicagenic acid.
176
177 Finally, medicagenic acid and its hepatic biotransformation products were subjected to
178 the *in vitro* crystallization assay to assess a possible inhibiting effect of metabolites of *H.*
179 *hirsuta* on crystal formation. Due to solubility issues, medicagenic acid was tested at a
180 final concentration of 0.2 mM in DMSO.
181
182 Crystal-cell interaction studies
183 When damage is applied to the intact renal epithelium, proliferation and migration of cells
184 bordering the wound is observed, entailing flattening and dedifferentiation of migrating
185 cells. Crystals preferentially bind to the surface of dedifferentiated and unpolarized cells,
186 enhancing the probability of urinary stone retention (Thongboonkerd et al., 2006).
187 Verkoelen et al. (1998) investigated the wound healing process and claimed that the level
188 of crystal binding increases tenfold immediately after damage is applied to the monolayer
189 with maximal crystal binding at wound closure. The retention of crystals on injured
190 monolayers was studied on damaged monolayers in presence or absence of modulators.

191 The effect was statistically evaluated using one-way ANOVA with Tukey post-hoc-test
192 (IBM SPSS Statistics version 27).
193
194 MDCK I cells were cultured in DMEM supplemented with 10% fetal bovine serum and
195 1% penicillin-streptomycin at 37 °C in a humidified atmosphere of 5% CO_2 in air. Cells
196 were seeded at a density of 1.1 x 10^5 cells.cm^{-2} on 24 mm polyester membrane filter
197 inserts (Transwell, 0.4 µm pore size (Corning, Tewksbury, United States)) to obtain
198 monolayers with a high level of differentiation. The medium volume was 2.5 mL in the
199 basal compartment and 1.5 mL in the apical compartment and medium was refreshed
200 every other day. Cultures were routinely checked for mycoplasma contamination and
201 found to be negative in all experiments. To study the effect of epithelial damage on crystal
202 adherence, the monolayer was injured. Strips of cells were scraped from the monolayer,
203 using the tip of a sterile 10 mL pipette. Two perpendicular scratches were made to create
204 a cross-shaped wound, with an approximate area of 1/3 of the total area (Verkoelen et al.,
205 1998).
206
207 72 h post-injury wounds were morphologically closed and culture medium was replaced
208 by buffer A (140 mM NaCl, 5 mM KCl, 1.5 mM $CaCl_2$, 0.5 mM $MgCl_2$, 50 mM urea, pH
209 6.6) in the apical compartment and buffer B (124 mM NaCl, 25 mM $NaHCO_3$, 2 mM
210 Na_2HPO_4, 5 mM KCl, 1.5 mM $CaCl_2$, 0.5 mM $MgCl_2$, 8.3 mM D-glucose, 4 mM alanine,
211 5 mM Na acetate, 6 mM urea, and 10 mg.ml^{-1} BSA, pH 7.4) in the basal compartment.
212 Buffer A was representative for the tubular fluid and buffer B for renal peritubular
213 capillary plasma (Verhulst et al., 2003). CaC_2O_4 (calcium oxalate) crystals were provided
214 by Sigma-Aldrich (St. Louis, MI, USA) and suspended in CaC_2O_4-saturated water (1.49

215 g.L^{-1}). A volume of 50 µL crystal suspension (16 µg.cm^{-2}, 0.511 µmol.well^{-1}) was added
216 to the apical compartment and incubated for 60 minutes at 37 °C. As a positive control,
217 CaC_2O_4 crystals were added in absence of any modulator. As a negative control, no
218 crystals were added to the cells and as a blank, filters without cells and crystals were used.
219 For all conditions six replicates were included. After incubation filters were rinsed three
220 times with PBS to remove non-adhered crystals, transferred to a tube (Starstedt,
221 Nümbrecht, Germany) and 250 µL HNO_3 suprapur was added. Samples were vortexed
222 and incubated overnight at 60 °C with a loose cap. Afterwards, 1.75 mL H_2O was added
223 and samples were vortex mixed again before centrifugation for 5 min at 3500 rpm. A
224 volume of 1 mL supernatant was diluted five times in 0.1% La_2O_3. Calcium content was
225 measured using Flame Atomic Absorption spectroscopy (Flame AAS, Perkin-Elmer,
226 Analyst 400). The wavelength was set at 422.7 nm, spectral band width at 0.7 nm, hollow
227 cathode lamp current at 15 mA, oxidant flow at 10 L.min^{-1} and fuel flow of acetylene at
228 2.5 L.min^{-1}. To quantify the results, a calibration curve (0.1 ppm Ca^{2+} to 2.0 ppm Ca^{2+})
229 was constructed.
230
231 Different compounds were tested as reference modulator of crystal binding. First
232 experiments were conducted with citrate and EDTA, known for their ability to form a
233 complex with Ca^{2+} (Verplaetse et al., 1986). Literature reports a beneficial effect of both
234 compounds on crystal-cell binding by a significant detachment of COM crystals from
235 MDCK cells (Chutipongtanate et al., 2012). Citrate solutions of 0.682 mM, 3.41 mM and
236 6.82 mM in buffer A (final concentrations 0.0341 µmol.well^{-1}, 0.171 µmol.well^{-1} and
237 0.341 µmol.well^{-1}) were prepared, complexing 10%, 50% and 100% of Ca^{2+} respectively.
238 $[Ca\text{-}EDTA]^{2-}$ complexes were formed using a stock solution of 10.22 mM EDTA in

239 buffer A (final concentration 0.511 µmol.well^{-1}). A volume of 50 µL was added to each
240 well.
241
242 Aescin was used at two concentration levels. The first concentration was equal to the
243 concentration of EDTA tested, taking a 1-1 interaction into account, using a stock solution
244 of 51.1 mM aescin in DMSO. 10 µL was added to each well (final concentration 0.511
245 µmol.well^{-1}). Attention was paid to keep the final concentration of DMSO in the well
246 below 1% to avoid toxicity (Taub et al., 2002; Winburn et al., 2012). The second
247 concentration of aescin was based on the CMC, being 0.11 mM in H_2O (Geisler et al.,
248 2020; Penfold et al., 2018). A stock solution of 16.5 mM aescin in DMSO was prepared
249 and 10 µL was added to the respective wells (final concentration 0.165 µmol.well^{-1}).
250
251 Finally, medicagenic acid and its hepatic biotransformation products were subjected to
252 the *in vitro* crystal-cell interaction assay to assess a possible effect of metabolites of
253 *Herniaria hirsuta* on crystal binding. Medicagenic acid was tested in a final concentration
254 of 0.511 µmol.well^{-1}, dissolved in DMSO, in accordance with EDTA and aescin. The
255 sample of hepatic metabolites of medicagenic acid was redissolved in buffer A. The
256 concentration of the most abundant metabolite present in the sample was estimated with
257 regard to the concentration of medicagenic acid before hepatic biotransformation,
258 resulting in an approximate final concentration of 0.0375 µmol medicagenic acid
259 glucuronide per well (Peeters et al., 2020b).
260
261 Cytotoxicity assay

262 A LDH cytotoxicity detection kit (LDH Kit-WST, Sigma Aldrich, St. Louis, USA), based
263 on the release of LDH into the culture supernatant upon damage of the plasma membrane,
264 was used to determine cytotoxic potential of modulators. An increase in dead or plasma
265 membrane-damaged cells results in an increase of LDH enzyme activity in the culture
266 supernatant, measured by the amount of formazan formed. A volume of 100 µL cell-free
267 culture supernatant is collected, mixed with 100 µL reaction mixture, containing
268 diaphorase (catalyst), NAD+, iodotetrazolium chloride and sodium lactate, and incubated
269 for 30 minutes at 37 °C. The maximum amount of releasable LDH enzyme activity is
270 determined by lysing the cells with a lysing solution (high control). LDH activity released
271 from untreated normal cells or spontaneous LDH release is defined using cells and assay
272 medium, without the test substance (low control). A background control is performed to
273 estimate the LDH activity in the assay medium. The average absorbance is calculated and
274 the absorbance value of the background control is subtracted from each of these values.
275 The resulting values are substituted in the following equation:

276 $$\text{Cytotoxicity (\%)} = \frac{\text{high control - low control}}{\text{exp. value-low control}} \times 100$$

277

278 **Results and discussion**

279 Crystallization assay

280 Citrate was used as a positive control and was tested at 3 different concentration levels:
281 0.3, 0.5 and 0.7 mM (final concentrations). Only the concentrations of 0.5 mM and 0.7
282 mM affected the crystal formation process in a significant manner. Citrate affects the
283 nucleation phase by complexing Ca^{2+}, with an inhibition percentage of (31.51 ± 10.00)%
284 and (66.60 ± 21.45)% and p-values of 0.04 and 0.00 respectively for 0.5 mM and 0.7 mM
285 (Figure 3). The effect on the aggregation phase was neglectable as the 95% confidence

286 interval included the point 0 (Figure 3). On the contrary, presence of aescin affected the
287 aggregation phase with an inhibiting effect of (190.97 ± 24.31)% and (260.25 ± 59.41)%
288 for 0.35 mM and 0.7 mM (final concentrations) respectively (Figure 3). Only 0.7 mM
289 aescin was statistically significant with a p-value of 0.03. Moreover, at a final
290 concentration of 0.35 mM, aescin trended to act as a promotor of crystal nucleation
291 resulting in more and smaller crystals. DMSO was evaluated as vehicle and showed no
292 influence on crystal formation rates.
293
294 Medicagenic acid 0.2 mM did not show a significant effect on nucleation of CaC_2O_4
295 crystals whereas aggregation was trended to be slightly promoted, implying that the
296 aglycon assists in forming larger aggregates of crystals. Overall, no significant effect on
297 nucleation or aggregation phase was observed, implying that the most abundant aglycon
298 present after gastrointestinal biotransformation of the *H. hirsuta* extract is not responsible
299 for the beneficial effect of the *H. hirsuta* extract on CaC_2O_4 crystal formation.
300
301 In agreement with aescin, the sample of hepatic metabolites of medicagenic acid also did
302 not significantly affect nucleation. This result is in contrast to earlier findings of Atmani
303 and Khan (2000), who reported promotion of nucleation. However, the research of
304 Atmani and Khan was performed *in vitro* on the herbal extract of *H. hirsuta* and did not
305 take into account biotransformation of the compounds. On the other hand, a trend towards
306 inhibition of aggregation by the hepatic metabolites of medicagenic acid was observed,
307 resulting in smaller CaC_2O_4 crystals in comparison with standard conditions. These
308 results are consistent with those of Atmani and Khan. Nevertheless, the inhibition of
309 aggregation is not significant and less pronounced compared to aescin. This lower effect

310 might be related to the lower concentration of the hepatic metabolites of medicagenic acid
311 compared to aescin.
312
313 It should be taken into account that the final concentration of medicagenic acid
314 glucuronide is ten times lower than the tested concentration of medicagenic acid. For this
315 assay 3 mL of hepatic biotransformation products was purified, dried and redissolved in
316 40 µL DMSO. In order to reach the same concentration range as the model compounds,
317 30 mL of hepatic biotransformation products should be purified and dried, which is
318 impossible to redissolve in 40 µL DMSO. As previous research by Hess et al. (1995) and
319 Atmani and Khan (2000) did not show a linear relation between concentration of
320 modulator and inhibition of crystal formation, results cannot be extrapolated. This
321 practical limitation hampers comparison of the effect of the hepatic biotransformation
322 products of medicagenic acid to the other modulators. Nevertheless, a tentative effect on
323 crystal aggregation of the hepatic metabolites of medicagenic acid could be demonstrated
324 for the first time. The limiting effect on aggregation of crystals results in smaller particles
325 which are more easily excreted and might contribute to the beneficial effect of *H. hirsuta*
326 against urinary stones.
327
328 Crystal-cell interaction studies
329 Crystal binding on MDCK I cells was evaluated in presence and absence of citrate and
330 EDTA, known for their ability to complex Ca^{2+} and compared to the amount of Ca^{2+} in
331 absence (negative control) and presence (positive control) of COM crystals (Figure 4).
332 Despite the widespread use of oral citrate therapy for prevention and treatment of calcium
333 oxalate stones, no significant influence on crystal binding was observed (Phillips et al.,

334 2015). Although literature reports a significant reduction of adherent COM crystals to
335 MDCK cells by citrate and EDTA, these results could not be repeated here
336 (Chutipongtanate et al., 2012). However, previous work by Chutipongtanate et al. (2012)
337 was performed on MDCK cells, without specifying the strain. Using MDCK I cells, only
338 distal tubule cells and collecting duct cells were taken into account, representing the place
339 where CaC_2O_4 stones are expected *in vivo* (Verkoelen et al., 1998). This discrepancy in
340 cell lines used might be responsible for the conflicting results. Verplaetse et al. (1986)
341 reported solubility of 0.2 M COM in 0.08 M EDTA at pH 8 and 8.5, respectively 22.5
342 $g.L^{-1}$ and 24.5 $g.L^{-1}$. However, their results were observed after one week of shaking the
343 mixture, requiring longer incubation periods than relevant in *in vitro* and *in vivo*
344 experiments. Moreover, COM is the most thermodynamically stable and least soluble
345 CaC_2O_4 form.
346
347 Medicagenic acid, the most abundant aglycon after hepatic biotransformation, and aescin,
348 a model compound, were dissolved in DMSO before addition to the semi-permeable wells
349 containing MDCK I cells and CaC_2O_4. DMSO (final concentration 0.6% v/v) showed no
350 significant effect on crystal binding. However, an increased variation between the
351 replicates was observed. Medicagenic acid and aescin also showed no significant effect
352 on crystal binding, together with an increased variation between the replicates (Figure 4).
353
354 Despite no suitable modulator serving as reference for inhibition of crystal binding was
355 included, the hepatic biotransformation products of medicagenic acid were subjected to
356 the *in vitro* crystal-cell interaction assay and showed significant inhibition of crystal
357 binding to MDCK I cells compared to the positive control (absence of inhibitor) with a

358 p-value of 0.001. This inhibition was not observed for the blank hepatic samples,
359 indicating that the effect is caused by the metabolites and not due to matrix interference
360 (Figure 4).
361
362 Determination of cytotoxicity using the non-homogeneous LDH assay indicated that
363 increased variation was observed parallel with cytotoxic effects (Figure 5). Therefore, it
364 is hypothesized that MDCK I cells undergoing apoptosis release bound CaC_2O_4 crystals
365 which are eliminated during the washing steps. As it is unpredictable how many crystals
366 are bound to apoptotic cells, enlarged variation between the replicates can be expected
367 when cytotoxic effects are observed.
368
369 Literature reports that the amphiphilic structure of medicagenic acid glucuronide, with
370 carboxylic groups on both the hydrophilic part and the hydrophobic part of the molecule,
371 can have a dual effect on crystalluria, by complexing Ca^{2+} with carboxyl and/or hydroxyl
372 groups, and by enhancing the solubility of insoluble CaC_2O_4 aggregates in aqueous phases
373 by micelle formation. The carboxylic group of the hydrophilic glucuronide dissociates in
374 an aqueous solution and forms a carboxyl anion, increasing solubility of the compound
375 in an aqueous environment (Geisler et al., 2020; Stachulski & Meng, 2013). The
376 negatively charged hydrophilic part can complex with Ca^{2+}. Therefore, sugar moieties
377 with a -COOH functional group have a high potency for crystal binding (Song et al.,
378 2008). The absorption of medicagenic acid glucuronide on the crystal surface results in a
379 negatively charged ζ potential of the crystal surface. Negatively charged crystal surfaces
380 can improve the repulsive force among crystals and the negatively charged surface of a
381 damaged renal epithelial cell and inhibit crystal aggregation on the COM crystal surface,

382 thereby disrupting crystal growth, and inhibiting the formation of thermodynamically
383 stable COM crystals, while inducing and stabilizing metastable COD crystals (Huang et
384 al., 2017). This hypothesis is supported by previous research of Atmani et al. (2006) who
385 found more numerous and smaller crystals in presence of the *H. hirsuta* extract *in vivo*
386 with crystalluria mostly composed of COD, while COM was the most abundant form in
387 control rats. Thus, it is hypothesized that the most abundant metabolite of medicagenic
388 acid most likely has the potential to simultaneously eliminate both Ca^{2+} and insoluble
389 crystals via the urine, indicating that saponins containing medicagenic acid may act as
390 prodrugs.
391

392 **Conclusion**

393

394 For the first time, a tentative effect on CaC_2O_4 crystal aggregation of the hepatic
395 biotransformation products of medicagenic acid could be demonstrated *in vitro*.
396 Moreover, the hepatic biotransformation products of medicagenic acid showed significant
397 inhibition of crystal binding to MDCK I cells. As these effects affect both formation of
398 crystals by inhibiting aggregation and retention of crystals to renal tubular cells, it can be
399 stated that the beneficial effect of *H. hirsuta* against urinary stones may be attributed at
400 least in part to metabolites of medicagenic acid, indicating that saponins containing
401 medicagenic acid may act as prodrugs. Nevertheless, *in vitro* studies remain a simplified
402 approach to study urolithiasis. These results should be further confirmed by *in vivo*
403 studies, monitoring the metabolites in blood and urine after administration of a *Herniaria*
404 *hirsuta* extract.
405

Funding: This work was supported by Special Fund for Research of the University of Antwerp (Concerted Action), project ID no.30732

Conflict of interest:

We wish to confirm that there are no known conflicts of interest associated with this publication and there has been no significant financial support for this work that could have influenced its outcome.

413 **References**

414

415 Aggarwal, A., Singla, S., Tandon, C., 2014. Urolithiasis: Phytotherapy as an adjunct
416 therapy. Indian J. Exp. Biol. 53, 103-111.
417 Alelign, T., Petros, B., 2018. Kidney stone disease: an update on current concepts. Adv
418 urol. 1-18.
419 Ammor, K., Bousta, D., Jennan, S., Bennani, B., Chaqroune, A., Mahjoubi, F., 2018.
420 Phytochemical screening, polyphenols content, antioxidant power, and antibacterial
421 activity of *Herniaria hirsuta* from Morocco. Sci. World J., 7470384
422 Atmani, F., Khan, S., 2000. Effects of an extract from *Herniaria hirsuta* on calcium
423 oxalate crystallization in vitro. Bju. International. 85, 621-625.
424 Atmani, F., 2003. Medical management of urolithiasis, what opportunity for
425 phytotherapy. Front Biosci. 8, 507-514.
426 Atmani, F., Slimani, Y., Mimouni, M., Aziz, M., Hacht, B., Ziyyat, A., 2004. Effect of
427 aqueous extract from *Herniaria hirsuta* L. on experimentally nephrolithiasic rats. J.
428 Ethnopharmacol. 95, 87-93.
429 Atmani, F., Slimani, Y., Mbark, A., Bnouham, M., Ramdani, A., 2006. *In vitro* and *in*
430 *vivo* antilithiasic effect of saponin rich fraction isolated from *Herniaria hirsuta*. J. Bras.
431 Nefrol. 28, 199-203.
432 Butterweck, V., Nahrstedt, A., 2012. What is the best strategy for preclinical testing of
433 botanicals? A critical perspective. Planta Med. 78, 747-754.
434 Charrouf, Z., Nait-Mbark, A., Guillaume, D., Leroy, Y., Kol, O., 1996. Herniaria saponin
435 B, a novel triterpenoid saponin from *Herniaria fontanesii*, in: Saponins used in Food and
436 Agriculture, Springer, pp. 241-245.
437 Chutipongtanate, S., Chaiyarit, S., Thongboonkerd, V., 2012. Citrate, not phosphate, can
438 dissolve calcium oxalate monohydrate crystals and detach these crystals from renal
439 tubular cells. Eur. J. Pharmacol. 689, 219-225.
440 EMA/HMPC/554033/2018 EMA. Assessment report on *Herniaria glabra* L., *H. hirsuta*
441 L.,
442 *H. incana* Lam., herba. https://www.ema.europa.eu/en/documents/herbal-
443 summary/rupturewort-summary-public_en.pdf (accessed July 2021).
444 EMA/382941/2020 EMA. Rupturewort.
445 https://www.ema.europa.eu/en/documents/herbal-summary/rupturewort-summary-
446 public_en.pdf (accessed July 2021).
447 Geisler, R., Dargel, C., Hellweg, T., 2020. The biosurfactant β-aescin: A review on the
448 physico-chemical properties and its interaction with lipid model membranes and
449 Langmuir monolayers. Molecules. 25, 117.
450 Hess, B., Meinhardt, U., Zipperle, L., Giovanoli, R., Jaeger, P., 1995. Simultaneous
451 measurements of calcium oxalate crystal nucleation and aggregation: impact of various
452 modifiers. Urol. Res. 23, 231-238.
453 Hess, B., Jordi, S., Zipperle, L., Ettinger, E., Giovanoli, R., 2000. Citrate determines
454 calcium oxalate crystallization kinetics and crystal morphology—studies in the presence
455 of Tamm–Horsfall protein of a healthy subject and a severely recurrent calcium stone
456 former. Nephrol. Dial. Transplant. 15, 366-374.

457 Huang, L.-S., Sun, X.-Y., Gui, Q., Ouyang, J.-M., 2017. Effects of plant polysaccharides
458 with different carboxyl group contents on calcium oxalate crystal growth. Cryst. Eng.
459 Comm. 19, 4838-4847.
460 Mbark, A.N., Charrouf, Z., Wieruszeski, J.M., Leroy, Y., Kol, O., 1995. Herniaria
461 saponin A, a novel saponin from *Herniaria fontanesii*. Nat. Prod. Lett. 6, 233-240.
462 MBark, A.N., Guillaume, D., Kol, O., Charrouf, Z., 1996. Triterpenoid saponins from
463 *Herniaria fontanesii*. Phytochemistry. 43, 1075-1077.
464 Moe, O.W., 2006. Kidney stones: pathophysiology and medical management. Lancet.
465 367, 333-344.
466 Peeters, L., Van der Auwera, A., Beirnaert, C., Bijttebier, S., Laukens, K., Pieters, L.,
467 2020a. Compound characterization and metabolic profile elucidation after *in vitro*
468 gastrointestinal and hepatic biotransformation of an *Herniaria hirsuta* extract using
469 unbiased dynamic metabolomic data analysis. Metabolites. 10, 111-136.
470 Peeters, L., Vervliet, P., Foubert, K., Hermans, N., Pieters, L., Covaci, A., 2020b. A
471 comparative study on the in vitro biotransformation of medicagenic acid using human
472 liver microsomes and S9 fractions. Chem. Biol. Interact. 328, 109192.
473 Penfold, J., Thomas, R., Tucker, I., Petkov, J., Stoyanov, S., Denkov, N., 2018. Saponin
474 adsorption at the air–water interface—Neutron reflectivity and surface tension study.
475 Langmuir. 34, 9540-9547.
476 Phillips, R., Hanchanale, V.S., Myatt, A., Somani, B., Nabi, G., Biyani, C.S., 2015.
477 Citrate salts for preventing and treating calcium containing kidney stones in adults.
478 Cochrane Database of Syst. Rev.
479 Rule, A.D., Lieske, J.C., Li, X., Melton, L.J., Krambeck, A.E., Bergstralh, E.J., 2014. The
480 ROKS nomogram for predicting a second symptomatic stone episode. J. Am. Soc.
481 Nephrol. 25, 2878-2886.
482 Sharma, D., Dey, Y.N., Sikarwar, I., Sijoria, R., Wanjari, M.M., Jadhav, A.D., 2016, *In*
483 *vitro* study of aqueous leaf extract of *Chenopodium album* for inhibition of calcium
484 oxalate and brushite crystallization. Egypt. J. Basic Appl. Sci. 3, 164-171.
485 Song, S., Zhu, L., Zhou, W., 2008. Simultaneous removal of phenanthrene and cadmium
486 from contaminated soils by saponin, a plant-derived biosurfactant. Environ. Pollut. 156,
487 1368-1370.
488 Stachulski, A. V., Meng, X., 2013. Glucuronides from metabolites to medicines: a survey
489 of the *in vivo* generation, chemical synthesis and properties of glucuronides. Nat. Prod.
490 Rep. 30, 806-848.
491 Taub, M.E., Kristensen, L., Frokjaer, S., 2002. Optimized conditions for MDCK
492 permeability and turbidimetric solubility studies using compounds representative of BCS
493 classes I–IV. Eur. J. Pharm. Sci. 15, 331-340.
494 Theunis, M.H., Foubert, K., Pollier, J., Gonzalez-Guzman, M., Goossens, A., Vlietinck,
495 A.J., 2007. Determination of saponins in *Maesa lanceolata* by LC-UV: Development and
496 validation. Phytochemistry. 68, 2825-2830.
497 Thongboonkerd, V., Semangoen, T., Chutipongtanate, S., 2006. Factors determining
498 types and morphologies of calcium oxalate crystals: Molar concentrations, buffering, pH,
499 stirring and temperature. Clin. Chim. Acta. 367, 120-131.
500 van Dooren, I., Foubert, K., Bijttebier, S., Theunis, M., Velichkova, S., Claeys, M., 2016.
501 Saponins and Flavonoids from an Infusion of *Herniaria hirsuta*. Planta Med. 82, 1576-
502 1583.
503 Verhulst, A., Asselman, M., Persy, V.P., Schepers, M.S., Helbert, M.F., Verkoelen, C.F.,
504 2003. Crystal retention capacity of cells in the human nephron: involvement of CD44 and

its ligands hyaluronic acid and osteopontin in the transition of a crystal binding-into a nonadherent epithelium. J. Am. Soc. Nephrol. 14, 107-115.

Verkoelen, C.F., Van Der Boom, B.G., Houtsmuller, A.B., Schröder, F.H., Romijn,. J.C., 1998. Increased calcium oxalate monohydrate crystal binding to injured renal tubular epithelial cells in culture. Am. J. Physiol. Renal Physiol. 274, 958-965.

Verplaetse, H., Verbeeck, R., Verbaeys, A., Oosterlinck, W., 1986. Solubility of calcium oxalate monohydrate and hydroxyapatite in EDTA solutions. J. Urol. 135, 608-611.

Winburn, I.C., Gunatunga, K., McKernan, R.D., Walker, R.J., Sammut, I.A., Harrison, J.C., 2012. Cell damage following carbon monoxide releasing molecule exposure: implications for therapeutic applications. Basic Clin. Pharmacol. Toxicol. 111, 31-41.

517 **Figures**
518

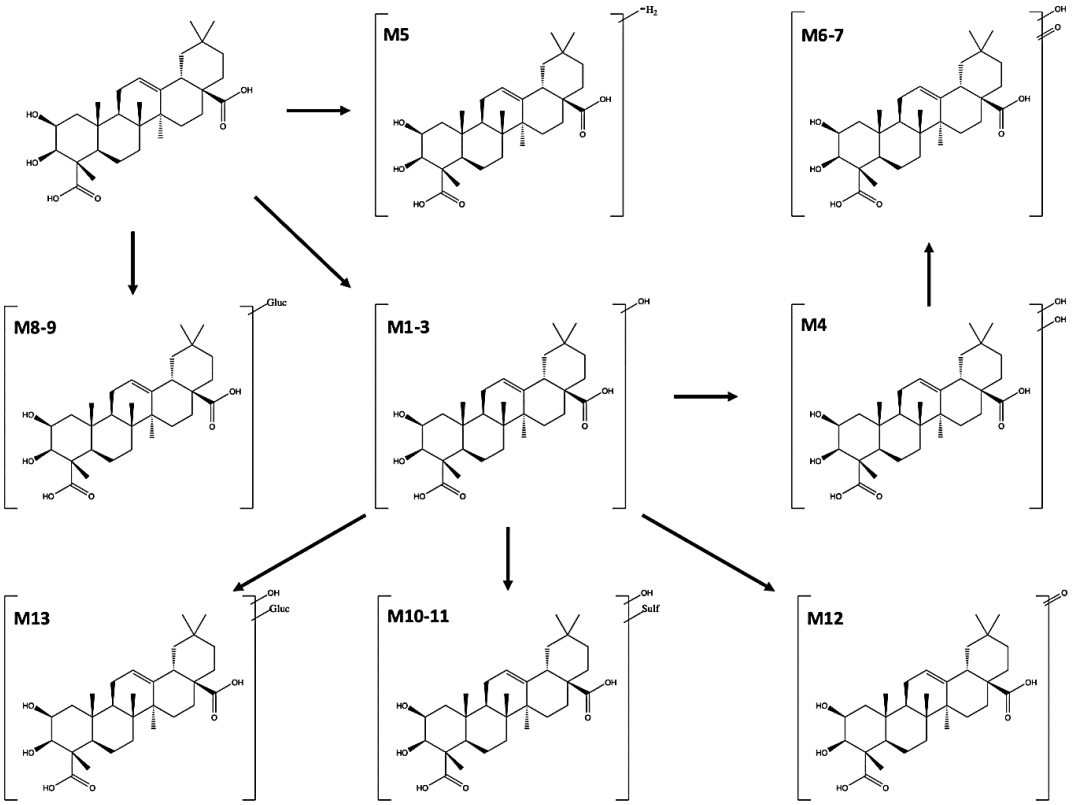

519
520 **Figure 1:** Suggested *in vitro* hepatic biotransformation pathway of medicagenic acid. Structural changes
521 due to biotranformation reactions are represented with OH (hydroxylation), =O (hydroxylation and
522 subsequent oxidation to keton), $-H_2$ (oxidation to keton), Gluc (conjugation with glucuronic acid) or Sulf
523 (conjugation with sulfate).

524
525

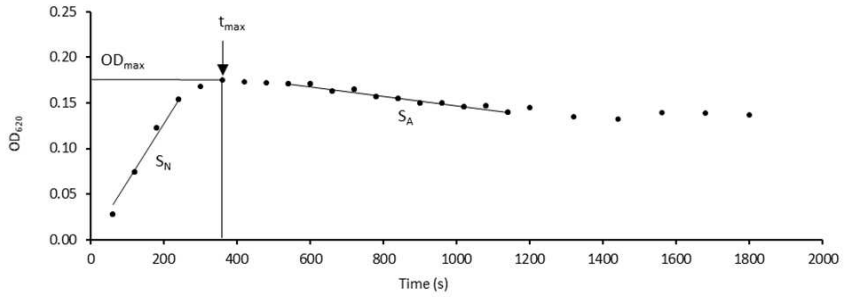

526
527 **Figure 2:** OD-curve, using a UV-VIS spectrophotometer (620 nm) after combining $CaCl_2$ and $Na_2C_2O_4$.
528 S_N: maximum slope of increase of OD_{620}, i.e. maximum rate of nucleation. S_A: maximum slope of decrease
529 of OD_{620}, i.e. maximum rate of aggregation. OD_{max}: maximum OD_{620} during nucleation, with t_{max} the
530 corresponding time. (Hess et al., 2000)

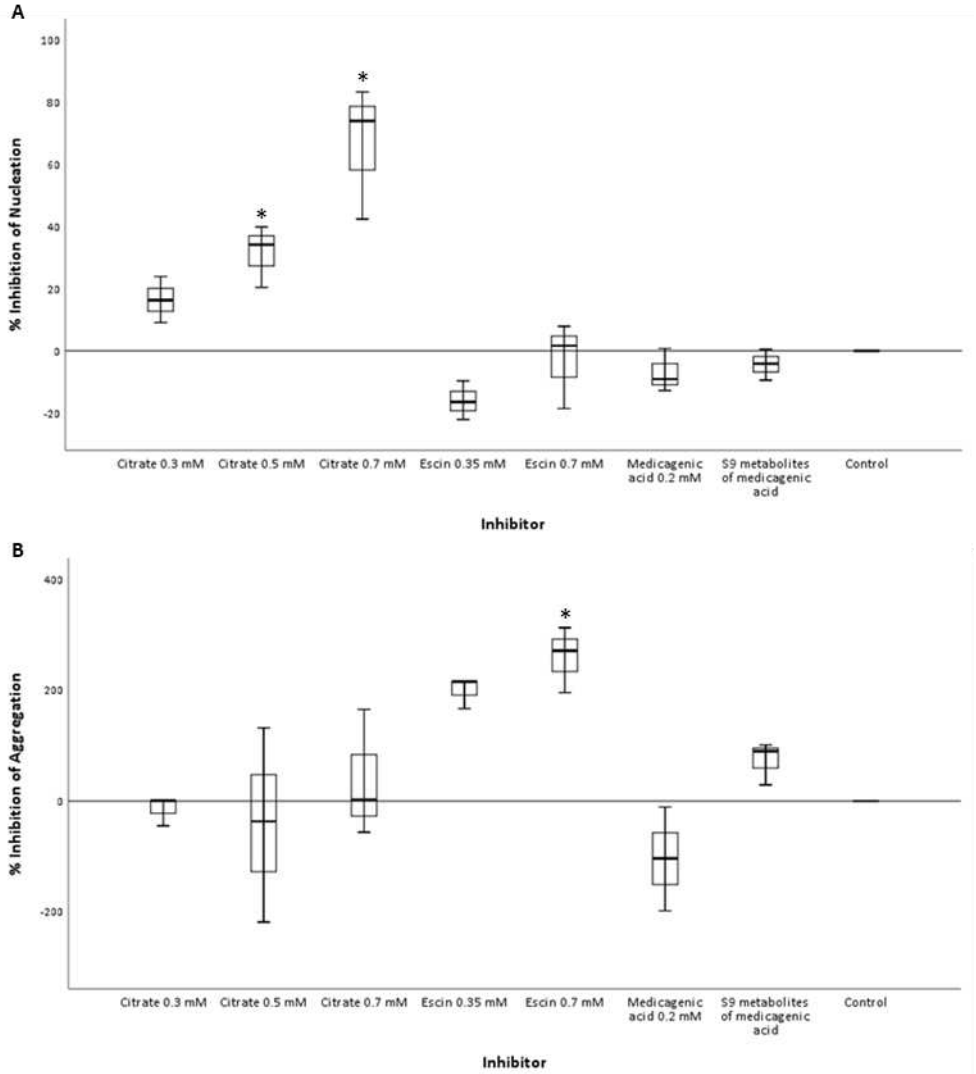

Figure 3: Inhibition of nucleation (S_N) and aggregation (S_A) of CaC_2O_4 crystals by citrate, aescin or medicagenic acid with and without hepatic biotransformation. * $p < 0.05$

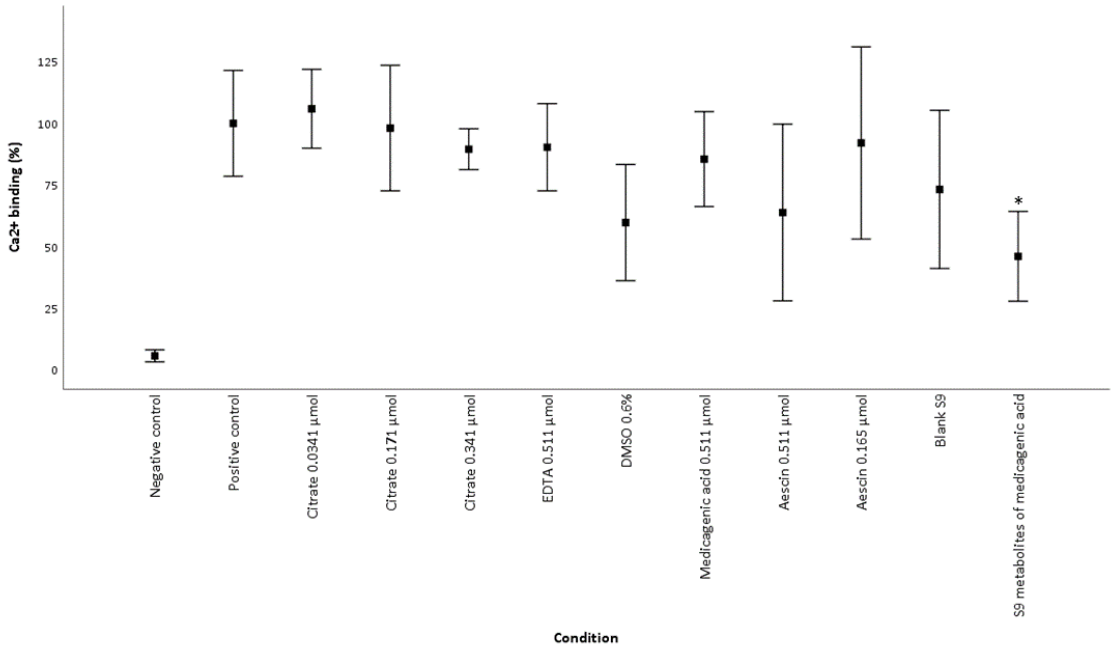

535

536 **Figure 4:** Ca^{2+} determination in absence (negative control) and presence (positive control) of COM
537 crystals and with addition of citrate 0.0341 µmol.well^{-1}, 0.1705 µmol.well^{-1} and 0.341 µmol.well^{-1}, EDTA
538 0.511 µmol.well^{-1}, medicagenic acid 0.511 µmol.well^{-1} and aescin 0.511 µmol.well^{-1} and 0.165
539 µmol.well^{-1} and with addition of medicagenic acid after and blank samples after hepatic
540 biotransformation. * $p < 0.05$

541

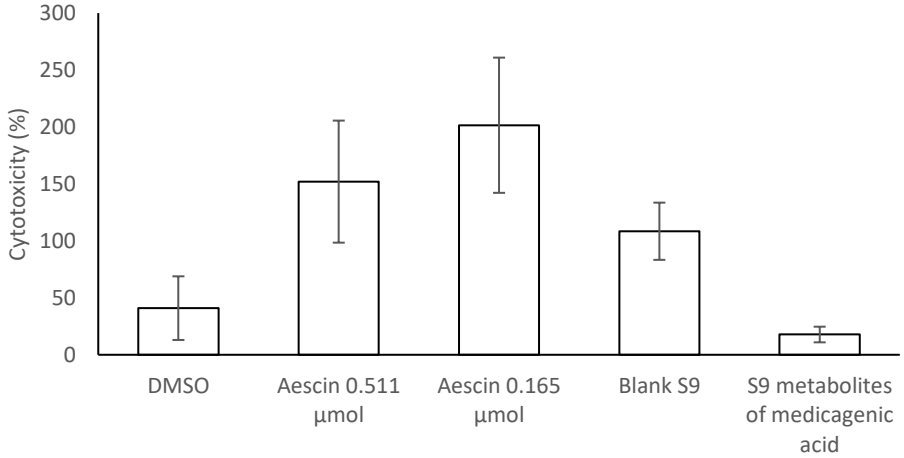

542

543 **Figure 5:** Cytotoxicity after 1 h of exposure to DMSO, aescin 0.511 µmol/well and 0.165 µmol/well, blank
544 hepatic samples and medicagenic acid after hepatic biotransformation.

545